13
Quantifying chaos with Lyapunov exponents

A. Wolf

The Cooper Union, School of Engineering,
Cooper Square, New York NY 10003, USA

13.1 Chaos, orbital divergence and the loss of predictability

Chaos has been discovered both in the laboratory and in the mathematical models that describe a wide variety of systems [1, 3]. In common usage chaos is taken to mean a state in which chance prevails. To the nonlinear dynamicist the word chaos has a more precise and rather different meaning. A chaotic system is one in which long-term prediction of the system's state is impossible because the omnipresent uncertainty in determining its *initial* state grows exponentially fast in time. The rapid loss of predictive power is due to the property that orbits (trajectories) that arise from nearby initial conditions diverge exponentially fast on the average. Nearby orbits correspond to almost identically prepared systems, so that systems whose differences we may not be able to resolve initially soon behave quite differently. In non-chaotic systems, nearby orbits either converge exponentially fast, or at worst exhibit a slower than exponential divergence: long-term prediction is at least theoretically possible.

Rates of orbital divergence or convergence, called Lyapunov exponents [2, 9, 13, 16], are clearly of fundamental importance in studying chaos. Positive Lyapunov exponents indicate orbital divergence and chaos, and set the time scale on which state prediction is possible. Negative Lyapunov exponents set the time scale on which transients or perturbations of the system's state will decay. In this chapter we define the spectrum of Lyapunov exponents, describe the well-known technique for computing a system's spectrum from its defining equations of motion, and outline a new technique for estimating non-negative exponents from experimental data.

13.2 **Quantifying chaos in a one-dimensional map**

The simplest chaos machine, the one-dimensional (1-D) map, is useful for illustrating the properties of Lyapunov exponents. One such map is the logistic equation, $x(n+1) = r*x(n)*(1-x(n))$, discussed in Chapter 3 [11]. $x(0)$ is an initial condition chosen in the interval (0,1), and r is a tunable parameter in [0, 4]. At $r = 4$ the trajectory (the sequence of map iterates $x(i)$, i = 0, . . .,∞) is known to be chaotic. In Fig. 13.1 the trajectories from two nearby initial conditions are seen to be diverging after only three iterations. If the two initial conditions are viewed as defining the error bar of some single *experimentally determined* initial condition, one's ability to pinpoint the system's state is clearly impaired after a few iterations. The reason for the growth of uncertainty is easily determined from the figure; the average slope of the map, as sampled by the trajectory, must be larger than one. An equivalent viewpoint is to consider the propagation of error through the map with a linear stability analysis. The error in specifying $x(n)$ is defined to be $dx(n)$, whereby

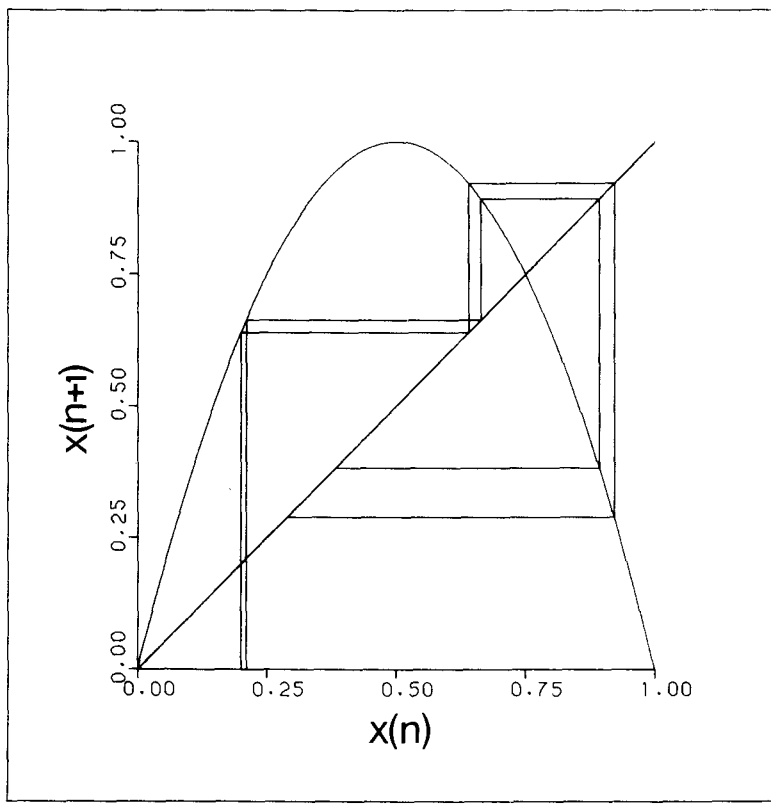

Fig. 13.1 A pair of nearby points is iterated through the logistic map, $x(n + 1) = 4*x(n)*(1-x(n))$. The resulting orbits diverge exponentially fast on the average. Map iteration consists of passing between the map and the line $x(n + 1) = x(n)$.

$$x(n+1)+\mathrm{d}x(n+1) = f[x(n)+\mathrm{d}x(n)] \sim f[x(n)]+\mathrm{d}x(n)*f'[x(n)] \quad (13.1)$$

$$\mathrm{d}x(n+1) = \mathrm{d}x(n)*f'[x(n)] = \mathrm{d}x(n)*r[1-2x(n)]$$

or, in terms of the initial uncertainty,

$$|\mathrm{d}x(n)| = |\mathrm{d}x(0)| * \prod_{i=0}^{n-1} |f'(x(i))| = |\mathrm{d}x(0)| * \prod_{i=0}^{n-1} |r(1-2x(i))| \quad (13.2)$$

For any value of r uncertainty tends to grow in time where the long-term product of the local stretching factors, $|r(1-2*x(i))|$, is greater than one.

If the uncertainty is to grow exponentially fast, eqn (13.2) must be consistent with

$$\mathrm{d}x(n) = \mathrm{d}x(0)*2^{\lambda n} \quad (13.3)$$

where λ is defined as the Lyapunov exponent. This requires that [13]

$$\lambda = \lim_{n\to\infty} \frac{1}{n} \sum_{i=0}^{n-1} \log_2|f'(x(i))|. \quad (13.4)$$

The limit of large n is necessary if we are to obtain a quantity that both describes long-term behaviour and is independent of initial condition. The limit effectively averages over all initial conditions, except perhaps for a negligible set of points (e.g. all of the points that eventually arrive at the unstable fixed point at the origin in the logistic equation). The probability density of the map is simply the normalised collection of delta functions that mark the locations $x(i)$ visited by a trajectory

$$p(x) = \lim_{n\to\infty} \frac{1}{n} \sum_{i=0}^{n-1} \delta(x-x(i)). \quad (13.5)$$

When combined with eqn (13.4) we obtain

$$\lambda = \int p(x)*\log_2|f'(x)|\,\mathrm{d}x \quad (13.6)$$

where the integral is taken over the domain of the map. The Lyapunov exponent is most easily understood in this form: local stretching, determined by the logarithm of the magnitude of the slope, is weighted by the probability of encountering that amount of stretching.

In Fig. 13.2 the Lyapunov exponent for the logistic equation is shown for r in (3.4, 4.0). As r is increased from 0 to approximately 3.57, the system exhibits a period-doubling sequence. At each r, the iterates $x(i)$ converge to a repeating sequence of period 2^n; n increasing by one at bifurcation points such as $r \approx 3.45$. Stable periodic orbits are characterised by negative Lyapunov exponents; bifurcation points correspond to orbits of marginal stability and therefore have zero exponents. For any specified

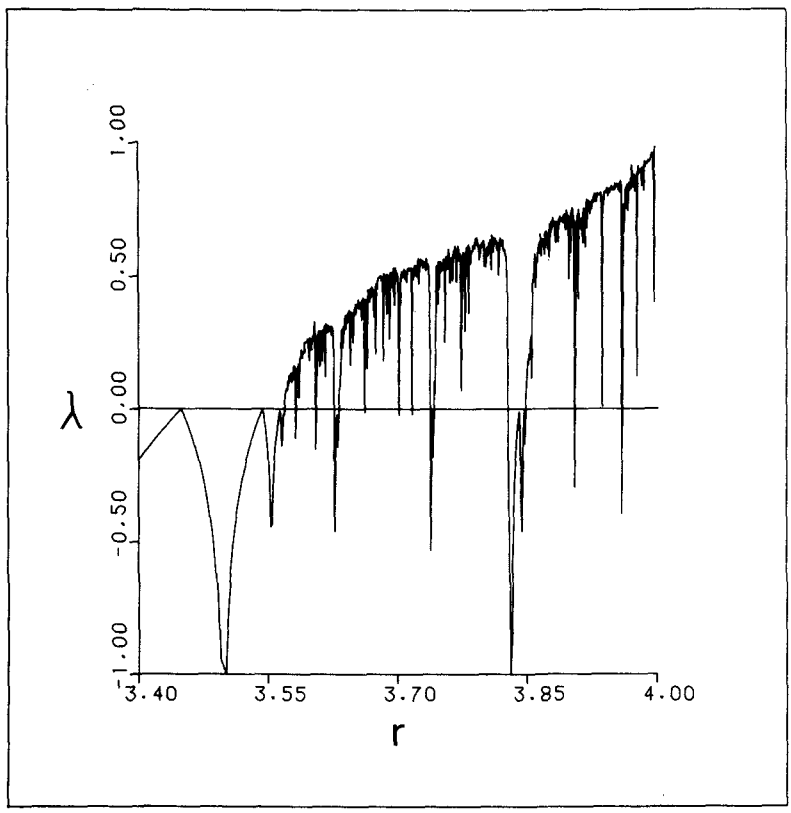

Fig. 13.2 The Lyapunov exponent for the logistic map is shown as a function of the parameter r. The curve for $r < 3.4$, which exhibits only the first period-doubling bifurcation, is not shown. The units of λ are bits of information lost per map iteration.

period there is a value of r where convergence is faster than exponential, and λ takes the value negative infinity. Only a few such superstable points, such as $r \approx 3.50$, can be resolved in Fig. 13.2. As r grows from 3.57 to 4.0, a trend towards increasingly chaotic behaviour and therefore a growing positive exponent is interrupted by an infinite number of 'windows' of periodic behaviour. Figure 13.2 concisely summarises the dynamics of the logistic equation as a function of its tunable parameter, though certain properties, such as the period of the periodic states, cannot be determined from the graph alone.

The units of λ are bits of information per map iteration. (The reader is cautioned that some authors define λ with $\log_e$ rather than $\log_2$ and then incorrectly use the units of (binary) bits per iteration.) For any r, and any specified precision of the initial condition, the value of λ read from the graph quantifies the average rate of loss of predictive power. For example,

at $r = 4$, $\lambda = 1.0$ bits per iteration. If an initial condition can be specified to 16 bits of precision, only 8 bits of state information remain after 8 iterations, 4 bits after 12 iterations, and predictive power is completely lost after 16 iterations. (The qualification that λ defines the *average* rate of loss of predictive power is an important one because the uncertainty interval may occasionally shrink for a few iterates if the slope of the map is not everywhere larger than one.) Knowledge of the system's state may be thought of as residing in a 16-bit shift register. At $r=4$, each map iterate has the effect of shifting one bit to the left, past the decimal point and into the void. Bits that come in from the right end to take their place are 'garbage' bits that depend only on the manner in which the iterate is determined. The Lyapunov exponent for a 1-D map is thus the rate at which bits are shifted through the 'state knowledge register ' [15]. The analogy of a shift register is not an idle one; with a suitable coordinate transformation, the logistic equation for $r = 4$ becomes the 'bit shift' map $x(n + 1) = 2*x(n)$ (modulus 1).

For the 1-D map, exponential separation is incompatible with motion confined to the unit interval unless a 'folding' process merges widely separated points. In the logistic equation, folding occurs when a pair of simultaneously iterated points fall on opposite sides of $x = 1/2$. These points may be thrown very close together at which time orbital divergence loses (and then regains!) its exponential character. In the repeated stretching and folding that produces chaos, it is a local property of the flow, the stretching, that determines λ, and a larger scale property, the folding, that should never directly appear in exponent calculation. Avoiding the fold proves to be an important consideration in estimating Lyapunov exponents from finite quantities of experimental data. The existence of a fold suggests a modification of our earlier statement on orbital divergence; in chaotic systems, nearby orbits diverge exponentially fast on the average, *so long as their separation remains infinitesimal.* When analysing experimental data, the word 'infinitestimal' must be replaced with 'small compared to the range of dynamical motion'.

Given the functional form of a 1-D map or a long sequence of experimentally obtained map iterates, eqns (13.4) and (13.6) provide a means of estimating λ. This calculation is performed with experimental data for a chaotic chemical reaction governed by a 1-D map in Wolf and Swift [18], where the problems with this approach to estimating λ are discussed.

13.3 **Defining the Lyapunov spectrum**

For systems whose dimensionality is larger than one, there is a set or spectrum of Lyapunov exponents, each one characterising orbital divergence in a particular direction. The spectrum of exponents is first

described for the equations that arise from Lorenz's simple model of fluid convection [8].

$$\begin{aligned} \frac{dx}{dt} &= 16.0\,(y-x) \\ \frac{dy}{dt} &= 45.92x - xz - y \\ \frac{dz}{dt} &= xy - 4.0z \end{aligned} \tag{13.7}$$

In the three-dimensional 'phase space' defined by coordinates $(x(t), y(t), z(t))$, post-transient behaviour of almost all trajectories takes place on an 'attractor' whose appearance is locally nearly planar. In Figs. 13.3a–c the solution to these equations is shown for about 15 orbits as a dotted

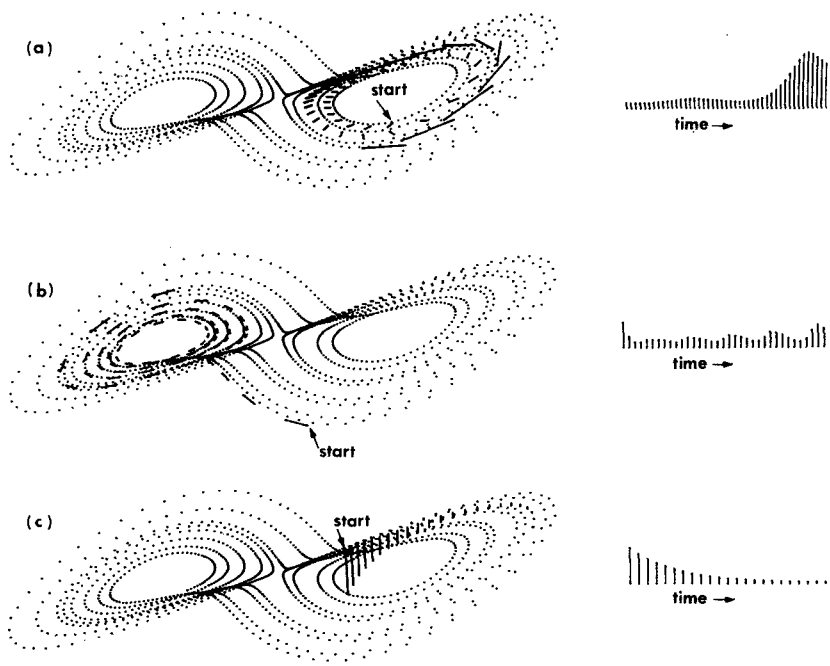

Fig. 13.3 The short-term evolution of the separation vector between three pairs of nearby points is shown for the Lorenz attractor. The true magnitude of the evolving vector appears to the right of each figure. (a) An expanding direction ($\lambda_1 > 0$). (b) A slower than exponential direction ($\lambda_2 = 0$). (c) A contracting direction ($\lambda_3 < 0$).

line. The Lorenz attractor is a 'strange' attractor as it is a chaotic system, possessing a positive Lyapunov exponent. In these figures three kinds of phase-space behaviour are displayed. In Fig. 13.3a an exponential divergence of two nearby points *on different orbits* in the attractor is shown. (It is possible to consider two points in the single long orbit defining the

attractor as being on different orbits, provided that their temporal separation is greater than a mean orbital period.) This chaotic motion is characterised by a positive Lyapunov exponent, λ_1. In Fig. 13.3b the behaviour of nearby points *on the same orbit* in the attractor is shown. The separation of these points neither grows nor shrinks exponentially fast so the associated Lyapunov exponent, λ_2, is zero. Finally, in Fig. 13.3c, the decay of a transient or perturbation to the attractor is illustrated. A point displaced off the attractor approaches a (carefully chosen!) point on the attractor, exponentially fast on the average. The associated exponent, λ_3, is negative. Lyapunov exponents involve long time averages, so the short segments of Fig. 13.3 will not accurately characterise the exponents; nevertheless, the qualitative behaviour is already visible. The complete spectrum of exponents for the Lorenz attractor is approximately (2.16, 0.0, –32.4) bits per second.

The three-dimensional phase space of the Lorenz attractor has three Lyapunov exponents, each describing the behaviour of one class of pairs of nearby orbits. In the general case, there are as many exponents as phase-space dimensions, though a particular Lyapunov exponent is not associated with a *unique* direction in phase space, such as a coordinate axis. For example, λ_3 describes orbital decay to the Lorenz attractor, motion orthogonal to the locally nearly planar attractor. However, the attractor is neither globally flat, nor exactly two-dimensional, so this direction varies in a complicated way over the attractor. λ_3 involves a long time average of the contracting nature of phase space over these directions.

The information theory interpretation of the Lyapunov exponents in the Lorenz attractor is a simple extension of the discussion for the 1-D map. If an initial condition is specified to 16 bits in each coordinate, the positive exponent of 2.16 bits per second means that all knowledge of the system's state (except that it still lies within the attractor) is lost after about 8 s, or about 16 mean orbital periods. If a perturbation appears in the next to least significant bit, the negative exponent of –32.4 bits per second means that the orbit will return to the attractor (to our resolution of 16 bits) in about one-sixteenth of an second, or about one-eighth of a mean orbital period.

All strange attractors in a three-dimensional phase space have the same spectral type, (+,0,–): a positive exponent indicating chaos within the attractor, a zero exponent for the slower than exponential motion along an orbit (ref. [5] contains a general proof of the existence of a zero exponent in continuous systems with strange attractors), and a negative exponent so that the phase space contains an attractor.

Even if the magnitudes of the Lyapunov exponents are not known, the spectral type provides a qualitative picture of a system's dynamics, as we have already seen for the logistic equation and the Lorenz attractor. A 1-D

map has a single exponent which is positive, negative or zero for chaotic, periodic, and marginally stable behaviour, respectively. In a three-dimensional continuous dissipative system, the only possible spectral types, and the attractors they describe, are: (+,0,–), a strange attractor; (0,0,–), a two-torus; (0,–,–), a limit cycle; and (–,–,–), a fixed point. In four dimensions there are three distinct types of strange attractor with spectral types: (+,+,0,–), (+,0,–,–), and (+,0,0,–).

The spectrum of Lyapunov exponents is now defined in a manner that is particularly useful for the algorithms later presented. Given a continuous dissipative dynamical system in an n-dimensional phase space, the long-term evolution of an infinitesimal n-sphere of initial conditions is monitored. Because of the deforming nature of the flow, the sphere will evolve into an n-ellipsoid. It is assumed that the centre of the sphere is *on* the attractor at $t = 0$, and that the principal axes of the ellipsoid have been ordered from most rapidly to least rapidly growing. The ith Lyapunov exponent is then defined in terms of the growth rate of the ith principal axis, $p_i(t)$

$$\lambda_i = \lim_{t \to \infty} \frac{1}{t} \log_2 \left[\frac{p_i(t)}{p_i(0)} \right] \tag{13.8}$$

Notice that the linear extent of the ellipsoid grows as $2^{\lambda_1 t}$, the area defined by the first two principal axes grows as $2^{(\lambda_1 + \lambda_2)t}$, the volume defined by the first three axes grows as $2^{(\lambda_1 + \lambda_2 + \lambda_3)t}$, and so on. This property provides an alternate definition of the spectrum of exponents: the sum of the first j exponents is given by the long-term exponential growth rate of the j-volume defined by the first j principal axes. This alternative definition will prove to be quite useful in spectral calculations. Whichever definition is employed, it is only necessary to follow the motion of as many points on the sphere as there are principal axes, although it may be easier to visualise phase-space behaviour if we consider the evolution of all points on the sphere's surface.

The existence of the limit in eqn (13.8) is not guaranteed for most of the model dynamical systems one is likely to encounter [2,9,13,16], and the situation for experimental data is even murkier. Calculations of orbital divergence rates necessarily characterise the properties of the given data set, and not necessarily the underlying dynamical system. We hope for some correspondence between these two sets of 'Lyapunov exponents', but in general it is not possible to independently confirm exponents determined from experimental data (however, see ref. [3]).

The behaviour of the evolving sphere of states is now examined. The centre of the sphere moves along the trajectory of some particular initial condition, while points on the surface of the sphere move along neighbouring trajectories. The sphere can therefore be expected to rotate and deform as it moves through phase space. Individual axes may grow or

shrink exponentially fast, or may show slower than exponential behaviour. The volume of the sphere decreases exponentially fast (as the sum of all of the Lyapunov exponents), but its linear extent grows exponentially fast (as λ_1). These two processes imply that the sphere becomes skewed exponentially fast. Should the sphere initially be finite in extent, each pass through the mandatory folding structure in the attractor would result in its being folded over on itself, ultimately evolving into an infinitely sheeted structure –an object with fractional dimension. Kaplan and Yorke [7] have established a method for estimating the fractional dimension of an attractor from a subset of the spectrum of Lyapunov exponents. When applied to the Lorenz attractor, a fractional dimension of 2.07 is obtained, confirming its not quite planar nature. If the initial sphere of states is infinitesimal in extent, the probability of encountering the fold is zero and the collection of states remains ellipsoidal for all time.

We now outline a proof that the sum of a system's Lyapunov exponents is the time-averaged divergence of its phase space, a quantity that is negative for the dissipative systems considered in this chapter. If a small volume element in a d-dimensional phase space, $\Delta V(t)$, grows exponentially fast with an exponent equal to the sum of all of the Lyapunov exponents, then

$$\frac{\mathrm{d}}{\mathrm{d}t}\Delta V(t) = \frac{\mathrm{d}}{\mathrm{d}t}\Delta V(0)2^{[\Sigma\lambda_i]t} = \Delta V(t)[\Sigma\lambda_i] \tag{13.9}$$

where a factor of $\log_e 2$ is ignored. The change in volume of the element is also given by

$$\begin{aligned}\frac{\mathrm{d}}{\mathrm{d}t}(\Delta x(t)\Delta y(t)\ldots) &= \Delta x(t)\Delta y(t)\ldots\left(\frac{1}{\Delta x(t)}\frac{\mathrm{d}\Delta x(t)}{\mathrm{d}t}+\frac{1}{\Delta y(t)}\frac{\mathrm{d}\Delta y(t)}{\mathrm{d}t}+\ldots\right)\\ &= \Delta x(t)\Delta y(t)\ldots(\Delta\dot{x}/\Delta x+\dot{y}/\Delta y+\ldots)\\ &= \Delta V(t)\,(\boldsymbol{\nabla}\cdot\mathbf{v})\end{aligned} \tag{13.10}$$

Comparing eqns [13.9] and [13.10] and noting that the former already involves a long time average, we obtain

$$\sum_{i=1}^{\mathrm{d}}\lambda_i = \overline{(\boldsymbol{\nabla}\cdot\mathbf{v})} \tag{13.11}$$

where the long time average may be taken over a single trajectory. We note that conservative systems may be chaotic, but cannot possess phase-space attractors.

13.4 Computing the Lyapunov spectrum from equations of motion

The calculation of the Lyapunov spectrum from the evolution of an infinitesimal state sphere may not be directly implemented on a computer, as computers cannot represent infinitesimal quantities. In a chaotic system, if the state sphere is initially finite, the exponentially rapid growth of its

linear extent means that the fold will be encountered long before the spectrum has converged: we fail to probe only the local structure of the attractor. An additional problem is the exponentially fast growth of the skewness of the sphere: principal axis vectors all collapse to the direction associated with the largest Lyapunov exponent, their directions becoming indistinguishable whatever the precision of one's computer. In Fig. 13.4 the evolution of a pair of initially orthogonal principal axis vectors (their size relative to the attractor greatly exaggerated) is shown in the Hénon strange attractor[6], which is generated by the two-dimensional mapping

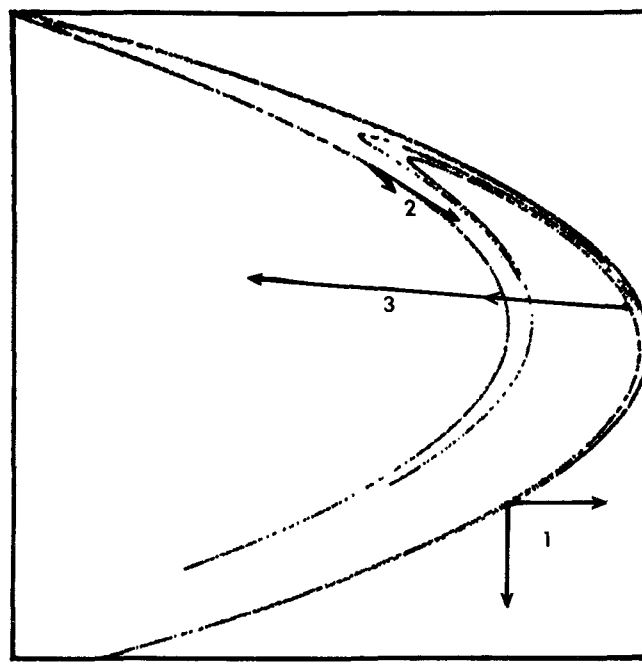

Fig. 13.4 The action of the Jacobian on an initially orthonormal pair of vectors is illustrated for the Hénon map: (1) initial vectors, (2) first iterate, and (3) second iterate. By the second iteration the divergences in extent and orientation are quite apparent. The angular orientations of the two vectors may be *numerically* resolved for a few more iterates.

$$x(n+1) = 1 + y(n) - 1.4*x(n)^2$$
$$y(n+1) = 0.3*x(n) \tag{13.12}$$

After only two iterates the linear extent and the skewness of the collection of states defined by the principal axis vectors are seen to be diverging. A solution to these problems was discovered independently by Bennetin *et al.*[2] and Shimada and Nagashima [16] in 1979. The result is a straightforward technique for computing a complete Lyapunov spectrum to any desired precision for systems whose equations of motion are available. This technique is now described in detail.

The solution to the divergent axis behaviour lies in the use of a technique from linear algebra, the Gram–Schmidt reorthonormalisation procedure, henceforth referred to as GSR [12]. Given a set of linearly independent vectors, GSR provides a new set of vectors that are orthonormal and preserve the orientation of various subspaces of the original set: the first vector in each set is identical in direction, the first two vectors in each set define the same plane, the first three vectors in each set define the same three-volume, and so on. These properties allow us to periodically replace the evolving ellipsoid with a new ellipsoid that is smaller (no problem of diverging extent) and whose principal axes have their orientation 'preserved' (we keep track of each phase-space direction) though the new axis vectors are all orthogonal (no orientation collapse).

We now review the Gram–Schmidt procedure. The first replacement vector is simply the first old vector, normalised. The second replacement vector is the second old vector with its component along the first new vector removed, then normalised. The third new vector is the third old vector with its components along the first two new vectors removed, then normalised, and so on. The reader can easily confirm the orientation preserving property of the replacement vector set from this description.

The importance of the orientation-preserving property of GSR is seen from the alternate definition of the spectrum of Lyapunov exponents, where the rate of length growth determines λ_1, the rate of area growth determines $\lambda_1 + \lambda_2$, and so on. Successive principal axis vectors define volume elements of all dimensions from one to that of the phase space, whose evolution may be simultaneously monitored. GSR allows the state sphere to be evolved for the long times required for exponent convergence because, though changing the directions of all but the first principal axis vector each time it is invoked, it never changes the orientation of any of the volume elements spanned by successive principal axis vectors. When GSR is used the initial and final volumes of the elements of each dimension $(L(t_j),\ L'(t_{j+1});\ A(t_j),\ A'(t_{j+1}); \ldots)$ are recorded and used to update running exponential growth rates. If m replacement elements spanning a time t have been used, the exponential growth rate of the first principal axis is

$$(\lambda_1)_m = \frac{1}{t} \sum_{j=1}^{m} \log_2 \left[\frac{L'(t_{j+1})}{L(t_j)} \right] \tag{13.13}$$

which is identical to the growth rate

$$\lambda_1 = \frac{1}{t} \log_2 \left[\frac{L'(t_1)}{L(t_0)} \right] \tag{13.14}$$

that would have obtained from the evolution of a single length element had we been able to follow it for time t. Similarly,

$$(\lambda_1 + \lambda_2)_m = \frac{1}{t} \sum_{j=1}^{m} \log_2 \left[\frac{A'(t_{j+1})}{A(t_j)} \right] \tag{13.15}$$

which is identical to the exponential growth rate of the area element defined by the first two principal axis vectors had we been able to follow it for a long time t. The expressions for the remaining exponents follow similarly.

To summarise the use of the Gram–Schmidt procedure, Lyapunov exponents will be computed from the long-term growth rates of volume elements of various dimensions. Elements may be replaced with smaller elements whose defining vectors are orthogonal, so long as the new elements have the same phase-space orientation as the ones they replace.

The technique described thus far requires that the nonlinear equations of motion be solved once for the centre of the sphere, and once for the end point of each principal axis vector, GSR being invoked when necessary. In a numerical implementation, GSR corresponds to integrating the differential equations for a new set of initial conditions that define the end points of the replacement vectors. The remaining practical difficulty is ensuring that GSR is performed frequently enough that only the local structure of the attractor is being probed.

The problem is avoided if we solve the nonlinear equations for the centre of the sphere, and simultaneously solve the *linearised* equations of motion about that point for each axis vector [2,16]. The linear system can only sample infinitesimal perturbations from the 'fiducial' trajectory of the centre point. This ensures that nearby orbits remain (relatively) near by for long times.

The use of the linear system appears to eliminate the need for GSR, at least for the divergence in the extent of the state ellipsoid. However, the linear equations diverge whenever there exists a positive Lyapunov exponent, just as the nonlinear equations do. The advantage of the linear system is that its solutions continue to represent infinitesimal deviations from the fiducial trajectory, even as they grow numerically large. The divergence in the linear system is simply a problem of exceeding the word size of one's computer: the solution remains small relative to the attractor. The role of GSR in the linear system is to prevent the orientation divergence, and simply to keep numbers manageable in size. More details about this calculation, as well as FORTRAN code for its implementation, may be found in ref. [19].

Although this calculation has been described for a set of ordinary differential equations, it is essentially unchanged if the system is defined by a discrete mapping such as the Hénon map. A linear stability analysis provides us with the linearised equations of motion: the Jacobi matrix for the map, whose evaluation requires iterating the nonlinear equations for the fiducial trajectory. The evolution of nearby orbits is determined by the

action of the Jacobian on principal axis vectors. Figure 13.4 shows the action of the Jacobian on a pair of principal axis vectors — not the evolution of three nearby initial conditions by the nonlinear mapping as was previously stated. The evolution of either principal axis vector in a single iteration is given by

$$(13.16)\qquad \begin{pmatrix} dx(n+1) \\ dy(n+1) \end{pmatrix} = \mathbf{J}_n \begin{pmatrix} dx(n) \\ dy(n) \end{pmatrix} = \begin{pmatrix} -2.8*x(n) & 1.0 \\ 0.3 & 0 \end{pmatrix} \begin{pmatrix} dx(n) \\ dy(n) \end{pmatrix}$$

so that

$$(13.17)\qquad \begin{pmatrix} dx(n) \\ dy(n) \end{pmatrix} = \mathbf{J}_{n-1} \left[\mathbf{J}_{n-2} \cdots \mathbf{J}_1 \begin{pmatrix} dx(1) \\ dy(1) \end{pmatrix} \right]$$

or, by regrouping the terms,

$$(13.18)\qquad \begin{pmatrix} dx(n) \\ dy(n) \end{pmatrix} = \left[\mathbf{J}_{n-1}\ \mathbf{J}_{n-2} \cdots \mathbf{J}_1 \right] \begin{pmatrix} dx(1) \\ dy(1) \end{pmatrix}$$

In eqn (13.17) the latest Jacobi matrix acts on the *current* axis vector, that vector reflecting the action of all previous Jacobi matrices on the *initial* axis vector. When divergences arise in the current vector pair, the pair is replaced. This is the same interpretation of the procedure of 'evolution and replacement' as was presented for the continuous system. In eqn (13.18) the action is contained in the product Jacobian which acts on the *initial* pair of axis vectors. Here divergences appear in the product Jacobian, either when its elements diverge, or its columns all converge to large multiples of the eigenvector for the largest eigenvalue (orientation collapse), resulting in a zero determinant. In this case GSR corresponds to a set of operations on the product Jacobian; removing large scalar multipliers of the matrix and performing row reduction with pivoting. In the first interpretation, λ_1 is determined from the exponential growth rate of the first vector and $\lambda_1 + \lambda_2$ from the growth rate of the area defined by both vectors. In the second interpretation the Lyapunov exponents are determined from the eigenvalues of the long time product Jacobian. For the Hénon map the spectrum of Lyapunov exponents is approximately (0.4, –1.6) bits per iteration for the parameter values of eqn (13.12).

13.5 **Estimating the Lyapunov spectrum for experimental data**

The spectral calculation of the last section appears useless for the problem of determining Lyapunov spectra from experimental data as it requires the equations of motion defining the system. As mentioned in section 13.2, in continuous systems governed by a discrete 1-D map, the extraction of discrete map data allows the estimation of the largest exponent by some conceptually simple, if numerically unstable algorithms [18]. There have also been attempts to estimate the dominant (smallest magnitude) negative

exponent from experimental data by measuring the mean rate of decay of induced perturbations.

Substantial progress has recently been made in the general problem of spectral estimation from experimental data [19]. Utilising the alternative definition of the Lyapunov spectrum, all of the non-negative Lyapunov exponents may be estimated for any system in which samples of a single dynamical observable are available. This algorithm has been used successfully on model systems with known spectra, and early calculations on experimental data obtained from chemical and hydrodynamic strange attractors are promising. The algorithm is now briefly described.

The well known technique of phase-space reconstruction with delay coordinates [14,17] makes it possible to obtain an attractor whose Lyapunov spectrum is identical to that of the original attractor, from discrete-time samples of almost any dynamical observable. Given the time series $x(t_i)$, the new attractor is defined by the trajectory $(x(t_i), x(t_i+T), x(t_i+2T),\ldots, x(t_i+(n-1)T))$. For sufficiently large n, and almost all time delays T, an embedding of the original attractor is obtained. In what follows we assume that an attractor has been successfully reconstructed in this manner.

The long-term exponential growth rate of a j-volume element in an attractor is governed by the sum of the first j Lyapunov exponents, provided that the volume of the element is small enough that the linear approximation applies. In computing spectra from sets of differential equations it was convenient to use the linearised system, the tangent space of the centre of the sphere, to satisfy this constraint. We saw, however, that the evolution of volume elements and GSR might be performed in *phase* space, a space that is accessible with experimental data. GSR is not exactly applicable to experimental data, as data points will not be found at the precise locations of the replacement vector set. Thus, with experimental data it is possible to define initially small volume elements of any desired dimension, follow their evolution for short times, and even replace them when necessary, but it seems that their orientation must be lost upon replacement.

In ref. [19] we show that the errors involved in using *almost* orientation-preserving replacement elements decay exponentially fast in time, and , if certain requirements are met, do not accumulate from one replacement to the next. For example, the relative error in estimating λ_1 is approximately $\theta_M{}^2/\lambda_1 t_r$ after many replacement and evolution steps, where θ_M is the maximum error in a single replacement and t_r is the time between replacements (the expression is only valid for rather large t_r). If it is possible to perform replacements infrequently, Lyapunov exponents may be accurately estimated from experimental data. The decay of orientation errors, that is, the approach of errant volume elements to the appropriate phase-space orientations, is guaranteed in a chaotic system, and the more

chaotic the system, the faster the decay. In the Lorenz attractor, a 20° orientation error in the replacement of each length element will result in a 10% error in λ_1, providing that replacements need not be performed more frequently than once per orbit.

We now discuss the particular case of estimating the sum of the first two Lyapunov exponents, which should illustrate the procedure for any number of exponents. Given an attractor reconstructed in n-dimensions, an area element is defined by three nearby points; the first delay coordinate point and its two nearest neighbours in n-space. If the three points were separated by at least one mean orbital period in the original time series, we may consider the points to have started from distinct initial conditions. The evolution of this element is monitored by simply looking ahead in the time series to find the future location of each of its defining points. When the triple begins to grow too large, or becomes so skewed that we expect to make a large error in computing its area (a problem that arises if external noise is present), we record the initial and final area of the current element, and then look for a replacement element. The search for replacements is somewhat involved, as it requires minimising both the size of the two replacement vectors, and the angular separation between the normals to the original and replacement elements. The initial area of the jth element is denoted by $A(t_j)$ and the element is replaced at time t_{j+1} when its area is $A'(t_{j+1})$ (see Fig. 13.5b). After m replacements spanning a long time t we estimate

$$(\lambda_1+\lambda_2)_m = \frac{1}{t}\sum_{j=1}^{m} \log_2\left[\frac{A'(t_{j+1})}{A(t_j)}\right] \tag{13.19}$$

This is identical to eqn (13.15) except that we are working in a reconstructed phase space with replacement elements that are always finite and only approximately orientation-preserving. In the limit of an infinite amount of noise-free data spanning an infinite number of orbits, this quantity is exactly the sum of λ_1 and λ_2. In practice, experimental data are noisy and span a finite number of orbits, so the accuracy of the estimate depends on the quality and quantity of experimental data. In Fig. 13.5a the algorithm for estimating λ_1 is presented schematically.

Despite the similarity of our algorithm to the calculation for model systems, it may not be used in general to determine negative exponents from experimental data. In systems such as the nearly planar Lorenz attractor, there is little or no *resolvable* fractal structure: thus we cannot define volume elements whose dimension is larger than that of the planar surface. Even in a system with resolvable fractal structure, such as the 1.26-dimensional Hénon attractor, areas decay much faster than lengths grow, so that area elements must be replaced with great frequency. Since post-transient attractor data are not effective for sampling contracting phase-space directions, it seems reasonable that the decay of induced

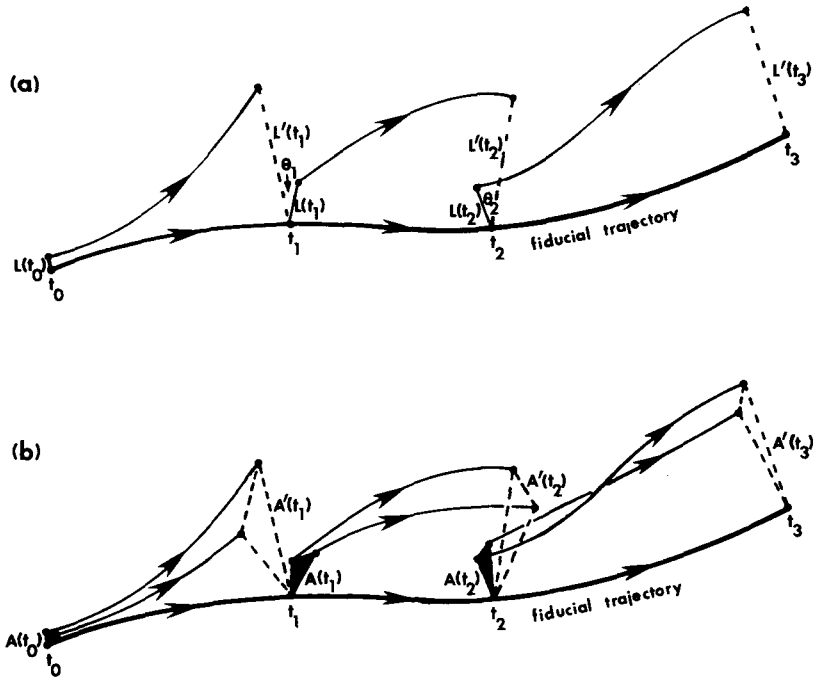

Fig. 13.5 A schematic representation of the procedure used to estimate Lyapunov exponents from experimental data. (a) The largest Lyapunov exponent λ_1 is computed from the growth of length elements. When the vector between the two data points has become large, a new point is chosen near the fiducial trajectory, minimising the replacement length L and the orientation error θ. (b) A similar procedure is followed to calculate $\lambda_1 + \lambda_2$ from the growth of area elements. When an area becomes too large or too skewed, two new points are chosen near the fiducial trajectory, minimising the replacement area A and the difference between the phase-space orientation of the original and replacement areas.

perturbations might provide a means of estimating negative exponents. This approach has several problems to contend with, of which the most important may be verifying that perturbations change only the state of the system (the current values of phase space variables) and not the system itself.

Our algorithm has been tested on many systems including the Hénon, Lorenz, and hyperchaos attractors (the last is a 3.005-dimensional attractor in a four-dimensional phase space with two positive Lyapunov exponents). The defining equations of motion were used solely to generate an observable sample of a one-dimensional coordinate projection. For these systems, the non-negative exponents were determined to within a few per cent of their known values. In ref. [3] we presented results for λ_1 for experimental data obtained from the Taylor-Couette hydrodynamic system as a function of the relative Reynolds number R/R_c. A transition to chaos from motion on a two-torus at $R/R_c \approx 12.2$ had already been suggested

by other dynamical diagnostics (phase portraits, Poincaré sections, power spectra, fractional dimension) but was first usefully quantified by the calculation of λ_1 (R/R_c).

A fundamental problem with the computation of Lyapunov exponents from experimental data is that the exponents are not rigorously defined in the presence of external noise. (See, for example, ref. [10].) Our calculations are based on the assumption that behaviour on (relatively noise-free) intermediate length scales is close to that on the smallest experimentally accessible (noise-dominated) length scales, which is assumed to be close to that on infinitesimal length scales in the (identically noise-free) underlying system. We have found that low-pass filtering of experimental data before exponent estimation has often reduced the effects of moderate amounts of external noise.

We conclude with the results of ref. [19] concerning data requirements. In each of the systems studied, 6 or 7 bits of data resolution sufficed for accurate exponent estimation. The number of data points required to estimate all of the non-negative exponents in a system of fractional dimension d is on the order of 10^d to 30^d, spanning between 10^{d-1} and 100^{d-1} orbits, where the value within these ranges depends on the complexity of the underlying 1–D map (if such a map exists). Exponent estimation appears to be prohibitively expensive for attractors of dimension greater than 3 or 4. The problem is the same one that arises in all of the currently popular techniques for estimating fractional dimension. To 'diagnose' a high-dimensional attractor, the attractor must be defined (filled out) with a number of points that depends *exponentially* on its dimension [4]. This problem appears insurmountable, but as the theory of dynamical diagnostics is incomplete, we are hesitant to proclaim such calculations impossible.

Acknowledgements

The author wishes to thank Jack B. Swift and Harry L. Swinney of the University of Texas Nonlinear Dynamics Laboratory for their contributions to this work. The efforts of Bob Hopkins and Paul Johnson in the preparation of the chapter are gratefully acknowledged. Financial support was provided by the Department of Energy, Office of Basic Energy Sciences contract DE-AS05-84ER13147.

References

[1] Abraham, N.B., Gollub, J.P. and Swinney, H.L. Testing nonlinear dynamics. *Physica 11-D,* 252–64 (1984), has an extensive list of references.

[2] Bennetin, G., Galgani, L. and Strelcyn, J-M. Lyapunov characteristic exponents for smooth dynamical systems and for Hamiltonian systems; a method for computing all of them. *Meccanica* **15**, 9–20 (1980).

[3] Brandstater, A., Swift, J., Swinney, H.L., Wolf, A., Farmer, J.D., Jen, E. and Crutchfield, J.P. Low-dimensional chaos in a hydrodynamic system. *Phys. Rev. Lett.* **51**, 1442–5 (1983).

[4] Greenside, H.S., Wolf, A., Swift, J. and Pignaturo, T. Impracticality of a box-counting algorithm for calculating the dimensionality of strange attractors. *Phys. Rev. A* **25**, 3453–6 (1982).
[5] Haken, H. At least one Lyapunov exponent vanishes if the trajectory of an attractor does not contain a fixed point. *Phys. Lett.* **94A**, 71–2 (1983).
[6] Hénon, M. A two-dimensional mapping with a strange attractor. *Comm. Math. Phys.* **50**, 69–77 (1976).
[7] Kaplan, J.L. and Yorke, J.A. Chaotic behaviour of multidimensional difference equations. In *Lecture Notes in Mathematics 730,* eds H.O. Peitgen and H.O. Walther. Springer, Berlin (1979).
[8] Lorenz, E.N. Deterministic nonperiodic flow. *J. Atmos. Sci.* **20**, 130–41 (1983).
[9] Lyapunov, A.M. Problème général de la stabilité du mouvement. *Ann. Math. Study* **17** (1947).
[10] Matsumoto, K. and Tsuda, I. Noise-induced order. *J. Stat. Phys.* **31**, 87 (1983).
[11] May, R. M. Simple mathematical models with very complicated dynamics. *Nature, Lond.* **261**, 459–67 (1976).
[12] Moore, J.T. *Elementary Linear and Matrix Algebra: the Viewpoint of Geometry*. McGraw-Hill, New York (1972).
[13] Oseledec, V.I. A multiplicative ergodic theorem. Lyapunov characteristic numbers for dynamical systems. *Trans. Moscow Math. Soc.* **19**, 197 (1968).
[14] Packard, N.H., Crutchfield, J.P., Farmer, J.D. and Shaw, R.S. Geometry from a time series. *Phys. Rev. Lett.* **45**, 712–16 (1980).
[15] Shaw, R. Modeling chaotic systems. In *Chaos and Order in Nature,* ed. H. Haken. Springer, Berlin (1981).
[16] Shimada, I. and Nagashima, T. A numerical approach to ergodic problem of dissipative dynamical systems. *Progr. Theor. Phys.* **61**, 1605–16 (1979).
[17] Takens, F. Detecting strange attractors in turbulence. In *Lecture Notes in Mathematics 898,* eds D.A. Rand and L-S. Young. Springer, Berlin (1981).
[18] Wolf, A. and Swift, J. Progress in computing Lyapunov exponents from experimental data. In *Statistical Physics and Chaos in Fusion Plasmas,* eds C.W. Horton, Jr. and L.E. Reichl, pp. 111–25 Wiley, New York (1984).
[19] Wolf, A., Swift, J.B., Swinney, H.L. and Vastano, J.A., Determining Lyapunov exponents from a time series. *Physica 16–D,* 285–317 (1985).